

Key Points:

- We use a novel method to make sea-level projections for global temperature pathways
- Median global sea-level projections for 1.5 and 2 degrees C in 2100 are 44 cm and 50 cm respectively
- Using a semi-empirical method, median global projections for 1.5 and 2 degrees C in 2100 rise to 58 cm and 68 cm

Supporting Information:

- Supporting Information S1

Correspondence to:

L. P. Jackson, luke.jackson@economics.ox.ac.uk

Citation:

Jackson, L. P., Grinsted, A., & Jevrejeva, S. (2018). 21st Century Sea-Level Rise in Line with the Paris Accord, *Earth's Future*, 6, <https://doi.org/10.1002/2017EF000688>

Received 20 SEP 2017

Accepted 15 JAN 2018

Accepted article online 24 JAN 2018

Abstract As global average sea-level rises in the early part of this century there is great interest in how much global and local sea level will change in the forthcoming decades. The Paris Climate Agreement's proposed temperature thresholds of 1.5°C and 2°C have directed the research community to ask what differences occur in the climate system for these two states. We have developed a novel approach to combine climate model outputs that follow specific temperature pathways to make probabilistic projections of sea-level in a 1.5°C and 2°C world. We find median global sea-level (GSL) projections for 1.5°C and 2°C temperature pathways of 44 and 50 cm, respectively. The 90% uncertainty ranges (5%–95%) are both around 48 cm by 2100. In addition, we take an alternative approach to estimate the contribution from ice sheets by using a semi-empirical GSL model. Here we find median projections of 58 and 68 cm for 1.5°C and 2°C temperature pathways. The 90% uncertainty ranges are 67 and 82 cm respectively. Regional projections show similar patterns for both temperature pathways, though differences vary between the median projections (2–10 cm) and 95th percentile (5–20 cm) for the bulk of oceans using process-based approach and 10–15 cm (median) and 15–25 cm (95th percentile) using the semi-empirical approach.

Plain Language Summary The sea level you experience at the coast can be estimated by the sum of contributions from ocean expansion, currents, ice melt from glaciers and ice sheets, land-water extraction/damming, and land motion. How sea level changes depends strongly on where you are because each contribution has a unique pattern. We use knowledge of these changes to make projections about future sea-level rise. We estimate how much sea-level could change if societies achieve either of the Paris Climate Agreement's temperature targets by 2100. If we reach 1.5°C or 2.0°C by 2100, GSL should rise around 44–50 cm, respectively. Using a slightly different method we find the global rise could be 58–68 cm. An incomplete picture of the sea-level components means that estimates could be out by up to 80 cm, though all projections show a sea-level rise of at least 20 cm.

1. Introduction

The Paris Climate Agreement (United Nations [UN], 2015a) aims to hold the rise in global average temperatures to “well below 2°C above preindustrial levels and to pursue efforts to limit the temperature increase to 1.5°C above preindustrial levels.” The agreement was signed by 195 countries and ratified by 170, equivalent to 87.9% of global emissions (Climate Analytics, 2017). While this outcome is highly encouraging, the process required to achieve deep and rapid emission reduction remains extremely challenging (Rogelj et al., 2016). A key question posed to the research community is the difference between the climate systems for these two temperature scenarios. At present, temperature pathways are an output of climate models for specific emissions scenarios rather than being the parameter under control.

While the atmospheric community have developed intercomparison projects to explore the impact of a Paris-like agreement upon, for example temperature and precipitation extremes (e.g., Mitchell et al., 2017), such intercomparison projects have not been made by the oceanographic community. This leaves the sea-level community needing to make the best of currently available data and methods. Two recent approaches aimed at overcoming this problem use idealized temperature pathways to drive a simple semi-empirical global sea-level (GSL) model (Bittermann et al., 2017), and use a reduced complexity carbon cycle—climate model to derive temperature ensembles that are used to drive a temperature scaled regional sea-level model (Schleussner et al., 2016). Rasmussen et al. (2017)

© 2018 The Authors.

This is an open access article under the terms of the Creative Commons Attribution License, which permits use, distribution and reproduction in any medium, provided the original work is properly cited.

is currently exploring preexisting climate model temperature output to develop regional sea-level projections.

GSL change can be explained by the sum of five components: ocean expansion, glaciers, Greenland ice sheet, Antarctic ice sheet, and land-hydrology. Regional relative sea-level (RSL) change depends upon the spatial variability of local ocean processes (Yin et al., 2010), static-equilibrium effects related to the redistribution of ocean and land-ice/-water mass interactions (Mitrovica et al., 2011), and is measured relative to vertical land motion due to glacial-isostatic adjustment (GIA; Farrell & Clark, 1976), local tectonics, ground-water extraction, and sediment compaction.

There are two main approaches employed to project sea level; the process-based method and the semi-empirical method.

The process-based method combines projections of individual components that are either directly output from climate models or estimated from physical models driven by climate model output (e.g., Church et al., 2013; Slangen et al., 2014). Implementations of this method have been probabilistic (e.g., Grinsted et al., 2015; Jackson & Jevrejeva, 2016; Kopp et al., 2014; Le Bars et al., 2017), possibilistic (Le Cozannet et al., 2017), and emulating coupled to a simplified climate-carbon cycle model (Nauels et al., 2017).

The semi-empirical method assumes a change in GSL as an integrated response of the climate system. The approach uses simple, physically motivated relationships determined from observations of GSL and global average temperature (e.g., Grinsted et al., 2010; Kopp et al., 2016; Vermeer & Rahmstorf, 2009) or global radiative forcing (e.g., Jevrejeva et al., 2010). These relationships are then used to project GSL using temperature or radiative forcing scenarios. Recently, the semi-empirical approach has been extended to estimate the contribution to GSL from individual components (Mengel et al., 2016).

To assess the question of future sea-level states at different temperature thresholds, we make sea-level projections using the process-based method in a probabilistic framework (Jackson & Jevrejeva, 2016). We make use of the Coupled Model Intercomparison Project Phase 5 (CMIP5; Taylor et al., 2012) and assess which models from representative concentration pathway (RCP) 2.6 and 4.5 (Moss et al., 2010), have global average temperature pathways conforming to 1.5°C and 2°C by 2100. We then use outputs from the conforming models for projections of steric, dynamic and glacier sea-level components. We use empirical relationships between global average temperature and rates of surface mass-balance (SMB) for Greenland (Fettweis et al., 2013) and Antarctic (de Vries et al., 2014) ice sheets to estimate their contribution to GSL rise. As with Intergovernmental Panel on Climate Change [IPCC] (2013), we cannot establish a temperature dependent dynamic ice-sheet contribution and thus use those estimated for Greenland and Antarctica for RCP 2.6 (Church et al., 2013). Changes in land-water storage are scenario independent in IPCC (2013), thus we apply this estimate to both temperature pathways.

We extend our analysis by using a semi-empirical model (Grinsted et al., 2010) to project GSL driven by temperature pathways from each of the CMIP5 models corresponding to 1.5°C and 2°C. We use these GSL projections in combination with process-based steric, glacier and land-water storage components to estimate an alternative ice-sheet contribution. Partitioning this ice-sheet contribution into Greenland and Antarctica allows us to regionalize the GSL projections. We selected this particular semi-empirical model because it explores a wider range of uncertainties than alternative models.

We produce global and regional RSL projections over the 21st century for each of the temperature scenarios. We compare projections of GSL, RSL, and individual components between the two temperature pathways and the two approaches to explore uncertainty (process-based and semi-empirical).

2. Materials and Methods

2.1. Selecting Temperature Pathways

We use the CMIP5 archive of RCP scenarios to identify models with global mean temperature pathways reaching 1.5°C and 2°C above preindustrial levels over the period 2080–2100 (relative to 1986–2005 where temperature is 0.61°C above preindustrial level, Hartmann et al., 2013). Given that few models achieve exactly 1.5°C or 2°C, we assign specific temperature ranges (centered about the desired mean) for a particular time, which are scaled to represent temperature uncertainty proportional to its mean. To do this we assess the relationship between mean global temperature (μ_T) and uncertainty (σ_T , multiplied by

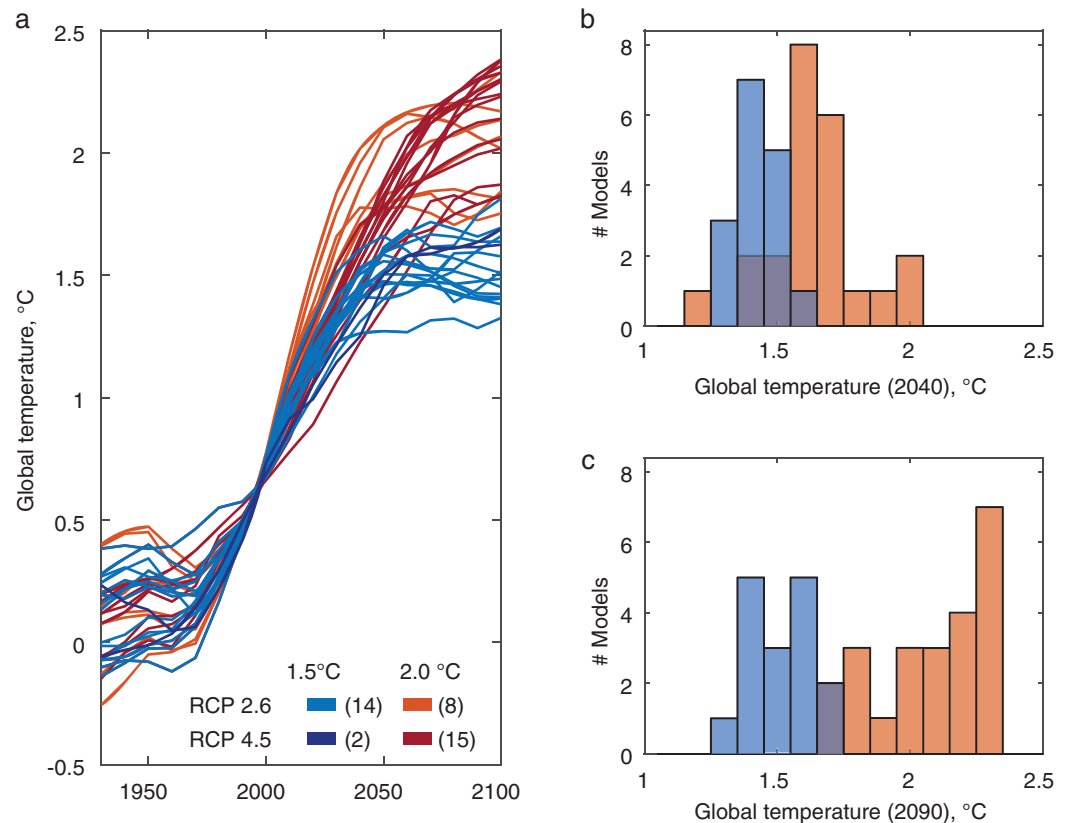


Figure 1. (a) Temperature pathways (relative to 1986–2005) of models from CMIP5 for RCP 2.6 and RCP 4.5 grouped by end-of-century temperature. (b) and (c) Histograms of model distribution for 1.5°C and 2.0°C subsets at 2040 and 2090. All temperatures shifted by 0.61°C (reference period relative to preindustrial, Hartmann et al., 2013).

1.65 to give 90% range) for the four RCP scenarios (we estimate multimodel ensemble mean and standard deviation) over the period 2080–2100 (Figure S1a, Supporting Information S1). We find a positive linear relationship with equation:

$$\sigma_T = 0.14\mu_T + 0.56. \quad (1)$$

Since there are only four data points it is difficult to justify the use of any higher order polynomial and a linear relationship is robust for both standard deviation ($R^2 = 0.96$) and variance ($R^2 = 0.92$). We optimize the uncertainty bounds by adjusting 1 so that the higher temperature (T_2) uncertainty is scaled by the mean temperature difference and the lower temperature (T_1) uncertainty:

$$\sigma_{T_2} = 0.14(\mu_{T_2} - \mu_{T_1}) + \sigma_{T_1}. \quad (2)$$

We tested a range of uncertainty bands for 1.5°C (Figure S1b) seeking a balance between large enough uncertainty bands to select a reasonable number of available models to estimate ensembles and small enough uncertainty bands to minimize their overlap to distinguish between the two temperature pathways. We select $\sigma_{1.5^\circ\text{C}}$ and $\sigma_{2.0^\circ\text{C}}$ of 0.21°C and 0.28°C, respectively, which results in 14 RCP 2.6 and 2 RCP 4.5 models for 1.5°C, and 8 RCP 2.6 and 15 RCP 4.5 models for 2.0°C (Figure 1).

We recognize that selecting subsets of models across RCP scenarios based upon their end-of-century relative temperature change is a subjective exercise. For this initial assessment, we briefly consider the statistical aspects of the distributions of all models for RCP 2.6 and RCP 4.5.

Using a standard Kolmogorov-Smirnov test (Massey, 1951) we find that neither the distribution of models for 1.5°C and 2.0°C at 2100 fail to reject the null-hypothesis of normally distributed models at the 5% significance level (P -values are 0.78 and 0.39, respectively). We thus take a standard “model democracy” approach

Table 1.
Subsets of CMIP5 Models Conforming to 1.5°C and 2.0°C

Model	1.5°C pathways		2°C pathways	
	RCP 2.6	RCP 4.5	RCP 2.6	RCP 4.5
BCC-CSM1-1	0.83			1.59
BCC-CSM1-1-m	0.82			1.51
BNU-ESM			1.14	
CanESM2			1.58	
CCSM4	0.87			1.64
CESM1-BGC				1.61
CESM1-CAM5			1.50	
CNRM-CM5	1.05			
CSIRO-Mk3-6-0			1.41	
EC-EARTH	0.93			
FIO-ESM		1.03		
GFDL-ESM2M	0.67			1.18
GFDL-ESM2G		1.00		
GISS-E2-H	0.79			1.69
GISS-E2-H-CC				1.38
GISS-E2-R				1.42
GISS-E2-R-CC				1.18
HadGEM2-AO	1.14			
HadGEM2-ES			1.45	
inmcm4				1.25
IPSL-CM5A-LR			1.22	
IPSL-CM5A-MR			1.12	
IPSL-CM5B-LR				1.64
MIROC5	1.03			1.71
MIROC-ESM			1.65	
MPI-ESM-LR	0.80			
MPI-ESM-MR	0.79			1.69
MRI-CGCM3	0.98			1.68
NorESM1-M	0.88			1.63
NorESM1-ME	0.99			
Average (# models)	0.91 ± 0.12°C (16)		1.47 ± 0.20°C (23)	
Average plus 0.61°C	1.52		2.08	

Note. Temperatures averaged from 2080 to 2100 shown for each model relative to 1986–2005 (add 0.61°C for ΔT , preindustrial to reference time).

(Knutti, 2010) with simple means and standard deviations of the model subsets. We reiterate that we use the CMIP5 models to explore sea-level change conditional upon temperature and that temperature pathways are a model output—the time-evolving emissions/concentrations of radiatively active constituents set by RCPs drive the model results (Moss et al., 2010).

2.2. Deriving GSL Components

Modeling sea level is a challenging proposition because the physical mechanisms and their interplay/dependence with/upon temperature are complex and exist at a variety of time scales.

GSL is affected by changes in ocean volume and changes in ocean mass. Ocean volume is affected by rising temperature and rising salinity that lead to an expansion and contraction of the ocean respectively, which at the global scale is dominated by ocean warming.

Ocean mass varies with the addition or removal of water by glaciers, ice sheets, and to a lesser extent human-land-water management (land-water storage, ground-water extraction, etc.). While present day

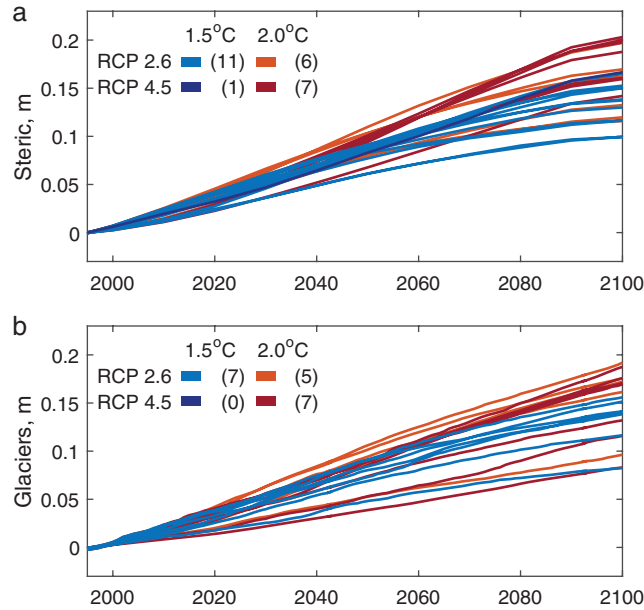


Figure 2. (a) Steric sea-level and (b) glacier contribution to GSL using available models corresponding to temperature pathways of models from CMIP5 for RCP 2.6 and RCP 4.5 with end-of-century levels of 1.5°C and 2°C.

estimates of mass-loss are consistent using a range of observation methods (e.g., Shepherd et al., 2012), and while modeling SMB has been successful using precipitation and temperature measurements for glaciers (e.g., Marzeion et al., 2012) and ice sheets (e.g., Fettweis et al., 2013), a knowledge gap exists in the dynamical contribution of ice sheets to sea-level change. This results in conservative GSL estimates using a process-based method (Le Bars et al., 2017).

We use the CMIP5 models in Table 1 for 1.5°C and 2°C (Figure 1a) that have global steric sea-level available to estimate an ensemble mean and uncertainty (Figure 2a). Similarly, we use available models for 19 glacial regions from Marzeion et al. (2012) (Figure 2b). We present two alternative approaches to estimate ice-sheet contributions to GSL in the next section.

We use a bootstrap method to capture uncertainty because of the limited number of available models for each temperature scenario. We estimate the 95th percentile of a 500 sample bootstrap for the model ensemble standard deviation at each time slice (and grid point for dynamic ocean processes).

The dependence of land-water storage/discharge upon temperature is much less clear. This is because human transformations of Earth's surface impact continental patterns of river flow and water exchange (Wada et al., 2017), and anthropogenic influence is more often driven by societal demand (Dalin et al., 2017). The uncertainty of land-water dependence is reflected in the same projected GSL contribution for all RCP scenarios in Church et al. (2013) (4 cm [−1 to 9 cm] by 2081–2100), which we use for both 1.5°C and 2°C scenarios.

2.3. Approaches to Calculate Ice-Sheet Contribution

2.3.1. Empirical Mass-Balance Model

We use the subsets of temperature time series to compute the SMB contribution of Greenland using the cubic relationship derived by Fettweis et al. (2013), which we convert to sea-level equivalent (1 mm GSL \approx 361.8 Gt):

$$\frac{dGRIS(t)_{SMB}}{dt} = -\frac{1}{361.8} (-71.5 \cdot \delta T(t)_{atm} - 20.4 \cdot \delta T(t)_{atm}^2 - 2.8 \cdot \delta T(t)_{atm}^3) \quad (3)$$

where $\delta T(t)_{atm}$ is global mean surface temperature at time, t relative to 1980–1999.

Similarly, we compute rates of SMB for Antarctica using the time and temperature dependent relationship used by de Vries et al. (2014):

$$\frac{dAIS(t)_{SMB}}{dt} = -\frac{1}{361.8} \cdot S_{ref} \cdot N_1 \cdot N_2 \int_{t_0}^t \delta T(t)_{atm} dt \quad (4)$$

where S_{ref} is the average SMB of Antarctica (183 ± 122 Gt) and $T(t)_{atm}$ is the global mean surface temperature. Both measurements are estimated relative to 1979–2010 (Lenaerts et al., 2012). N_1 and N_2 are

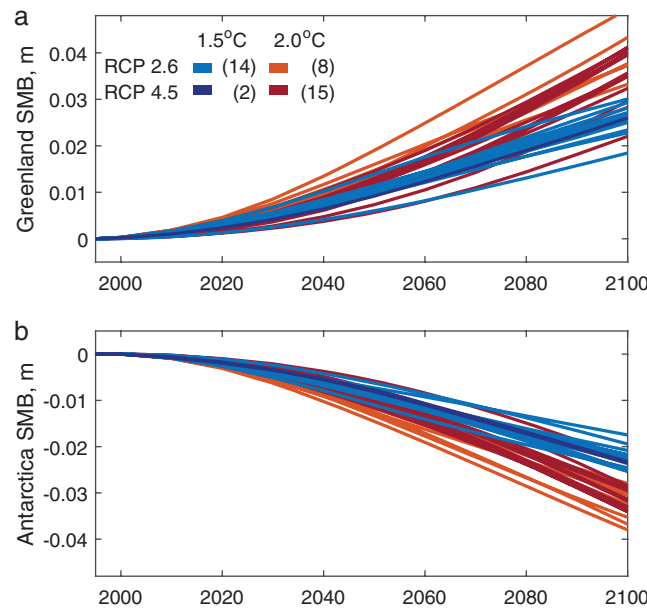


Figure 3. Surface mass-balance contribution to global sea-level for, (a) Greenland and (b) Antarctic ice sheets using available models corresponding to those projecting temperature (Figure 1).

the fractional precipitation increase with temperature ($5.1\% \pm 1.5\% [^{\circ}\text{C}]^{-1}$) and polar amplification ratio to global atmospheric temperature (1.1 ± 0.2). For Antarctica, we sample the range of parameter uncertainties to create a suite of possible SMB trajectories for a single model temperature pathway. We then calculate the mean of multiple trajectories for each model.

After estimating rates of SMB using 3 and 4, we integrate the result for each model and adjust the series so that they are relative to 1986–2005 (Figure 3).

Since the approach outlined here only estimates ice-sheet SMB, we incorporate rapid ice dynamics from Church et al. (2013) that contributes 4 cm [1–6 cm] and 7 cm [–1 to 16 cm] for Greenland and Antarctica, respectively. The ice dynamics component is invariant between scenarios in Church et al. (2013). While recent work simulating specific dynamic features shows a

strong dependence upon emissions scenario, strong mitigation (e.g., RCP 2.6) indicates a small ice-sheet dynamical contribution at least for those dynamic mechanisms included (DeConto & Pollard, 2016).

2.3.2. Semi-Empirical Sea-Level Model

To augment the empirical mass-balance calculation of the ice sheet (IS) contribution, we also use a semi-empirical sea-level model (Grinsted et al., 2010) to simulate GSL rise and then back-calculate the ice-sheet contribution. For each temperature subset (1.5°C and 2°C), each model temperature pathway is used to estimate future sea level from the semi-empirical model, giving a mean and uncertainty envelope. We then calculate the model-mean ensemble mean and model-uncertainty ensemble mean (Figure 4). We assume the validity of process-based contributions to GSL from steric, glacier and land-water components (STR, GLA, and LAN) to perform the back calculation:

$$IS = GSL - STR - GLA - LAN. \quad (5)$$

where we randomly sample each of the uncertainty envelopes of all components and solve 5 for each sample. We then use a ratio of 6:5 between Greenland and Antarctica sea-level contributions to partition the total ice-sheet contribution. This ratio is consistent with observations between 1992 and 2005 (e.g., Church et al., 2013; Shepherd et al., 2012).

2.4. Probabilistic Projections

We follow the same method as Jackson and Jevrejeva (2016) to make GSL and RSL projections. We create probability distribution functions (PDFs) to fit the percentiles of each global average contribution at each time slice. We sample these PDFs, and sum samples across components for each realization then estimate quantiles for GSL to establish a probabilistic projection. For RSL, we use the realizations of each global component to scale its associated normalized fingerprint. We sum across components at each grid point for each realization and then estimate quantiles to establish a probabilistic projection. We assume each of the sea-level components is uncorrelated (Jackson & Jevrejeva, 2016) and that the spatial pattern of future land-based mass loss will be the same as at present (Bamber & Riva, 2010).

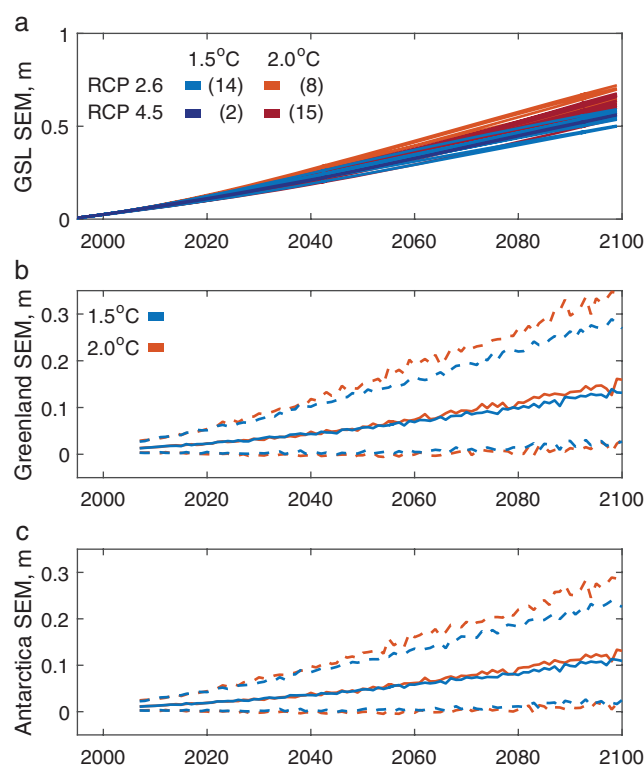


Figure 4. (a) Global sea-level projections using semi-empirical model for corresponding temperature pathways. Back-calculated contributions for (b) Greenland and (c) Antarctic ice sheets.

While the glacier, ice sheet and land-water components use a normalized fingerprint of RSL change, DSL (with net-zero GSL change, but significant nonzero spatio-temporal fields) is calculated at 10 year time slices as the multi-model ensemble mean of those CMIP5 models available for each temperature pathway.

There are three small changes made to the methodology compared to Jackson and Jevrejeva (2016). The first is that we estimate the global average projection from the global average components, rather than solving an area-weighted average of the regional projection. Second, we sample each PDF 5000 times rather than 1000 to improve the convergence and increase the number of samples drawn from the tails of the distribution. Third, we do not account for the impact of ocean self-attraction and loading (Richter et al., 2013), where ocean mass is redistributed from the deep ocean interior to shallow coastal regions as a result of volumetric expansion (Landerer et al., 2007). This effect alters sea level by less than 2 cm by 2100 for RCP 2.6 (Richter et al., 2013) as

estimated for the NorESM1-M model (Iversen et al., 2013).

3. Results

3.1. Global Projections

Figure 5 shows the probabilistic projections for GSL using the process-based approach of estimating temperature dependent sea-level components. The end-of-century median (5%–95% range) projected GSL is 44 cm (20–67 cm) and 50 cm (24–74 cm) for 1.5°C and 2°C pathways respectively. It certainly appears that there is little difference between projections using this approach, though the 1.5°C pathway has a slightly lower variance than for 2°C (47 versus 50 cm, respectively by 2100). Likewise the relative proportions of each component's variance to the total variance for each of the pathways are very similar, with the exception of glaciers, whose variance is greater for 2°C than 1.5°C.

In addition, Figure 6 shows the GSL projections using the semi-empirical approach to calculate ice-sheet contributions. The end-of-century median (5%–95% range) projected GSL is 57 cm (28–93 cm) and 68 cm (32–117 cm) for 1.5°C and 2°C pathways, respectively. The GSL projections thus differ markedly between the approaches used to calculate ice-sheet contributions. This is most obvious in the fraction of variance where the ice-sheets contribute 65%–70% of total uncertainty, which is consistent for the century (Figures 6c and 6d) compared to an increase from 10% to 50% over the century (Figures 5c and 5d) for the process-based approach to calculate ice-sheet contributions. Furthermore, the ratio between the contribution to uncertainty between Greenland and Antarctica is 1:4 (25:75) and 7:6 (54:46) for process-based and semi-empirical approaches of calculating ice-sheet contributions respectively. Interestingly, while we have forced the ice-sheet contributions with the semi-empirical method to have a fixed ratio of 6:5 (55:45) (e.g., Church et al., 2013; Shepherd et al., 2012), the ratio using the process-based approach varies between 49:51 and 56:44 over the course of the 21st century.

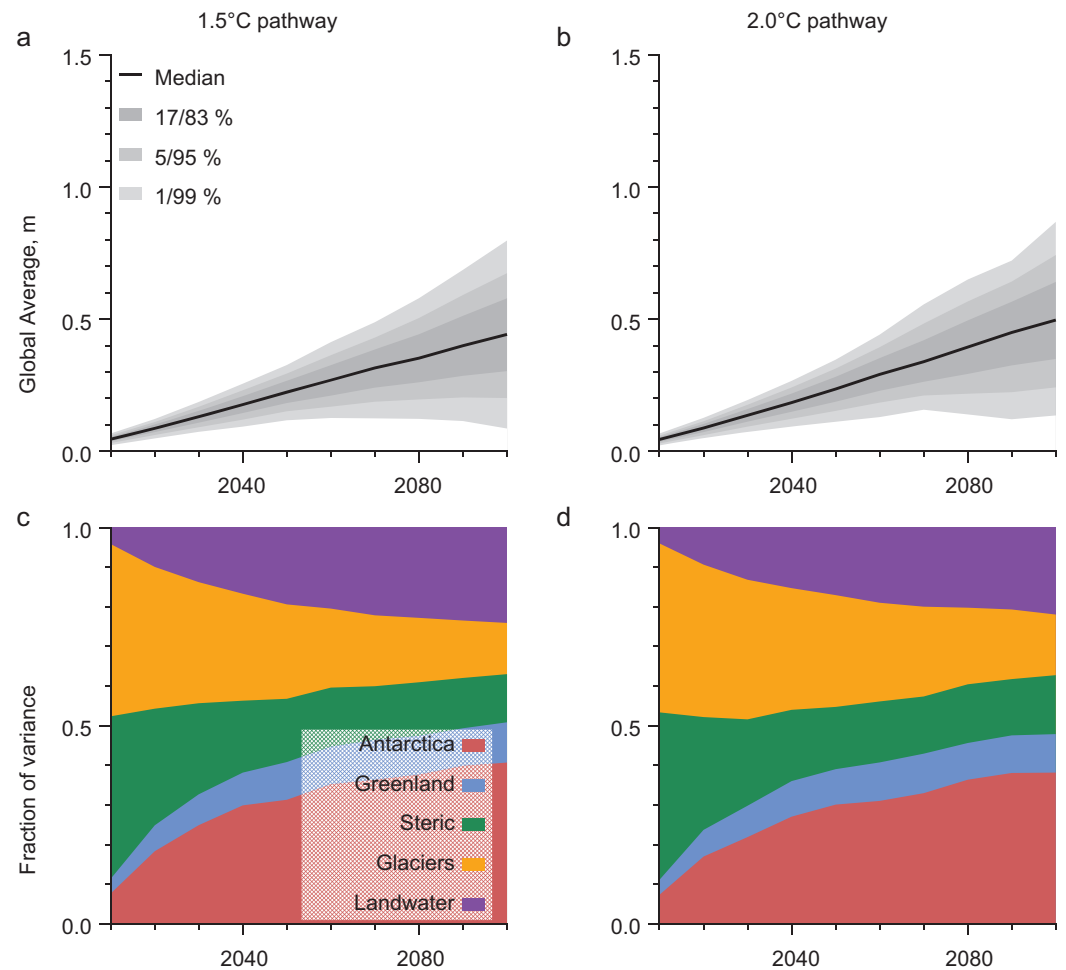


Figure 5. Global average sea-level projections (a) and (b) and fraction of variance of each sea-level component (c) and (d) for 1.5°C and 2°C temperature pathways using process-based approach to calculate ice-sheet contributions.

3.2. Regional Projections

Figures 7 and 8 show the RSL projections for 2100 and their associated uncertainties using the process-based and semi-empirical approaches respectively. Both projections include uplift from glacial-isostatic adjustment, which is a long-term pattern of land motion (and associated redistribution of ocean mass) due to the last deglaciation. We deem the rates of relative sea level associated with GIA to be constant at the multidecadal time scale (Peltier et al., 2015).

The patterns of all projections are similar for both temperature pathways and method of ice-sheet calculation. The differences between RSL for temperature pathways are 2–10 cm (median) and 5–20 cm (95th percentile) for the bulk of oceans using process-based approach (Figure 9) and 10–15 cm (median) and 15–25 cm (95th percentile) using semi-empirical approach (Figure 10).

4. Discussion

4.1. Comparison with Previous Work

We have made global (Table 2) and regional sea-level projections using process-based and semi-empirical approaches for 1.5°C and 2°C temperature scenarios. For the 1.5°C pathway we project median global sea level rise in 2100 of 44 cm and a 66% range of 30–58 cm (Table 2), both of which are in agreement with a median of 41 cm and 66% range of 29–53 cm by Schleussner et al. (2016). For the 2°C pathway we project median GSL rise in 2100 of 50 cm and a 66% range of 36–65 cm, which is almost identical to the median of 50 cm and 66% range of 36–65 cm by Schleussner et al. (2016). The results of Rasmussen et al. (2017), who

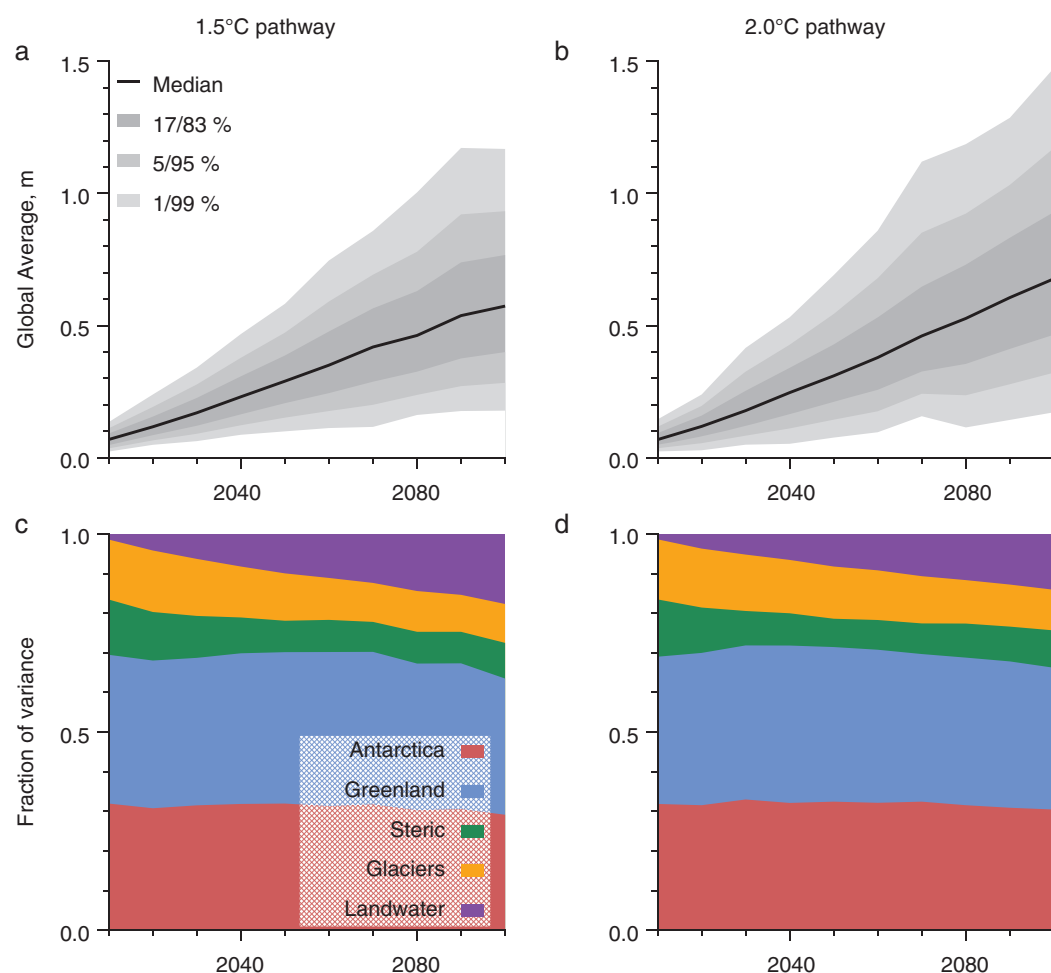


Figure 6. As in Figure 5 but using semi-empirical approach to calculate ice-sheet contributions.

use a very similar method (for temperature pathways and sea-level) to us, are currently in good agreement with ours.

In the case of our semi-empirical approach we project median global sea level rise in 2100 for the 1.5°C pathway of 57 cm and a 90% range of 28–93 cm (Table 2). While the median is in poor agreement with 34 cm by Bittermann et al. (2017) and 77 cm by Schaeffer et al. (2012), the range substantially overlaps with that of Bittermann et al. (2017) (23–58 cm) and Schaeffer et al. (2012) (54–99 cm). For the 2°C pathway we project median GSL rise in 2100 of 68 cm and a 90% range of 32–117 cm. Again, the median is in poor agreement with 46 cm by Bittermann et al. (2017) and 80 cm by Schaeffer et al. (2012) while the range fully encompasses that of Bittermann et al. (2017) (36–57 cm) and Schaeffer et al. (2012) (56–105 cm).

A larger range of projected median GSL change occurs in the semi-empirical results (Tables 2 and 3), which is due to a combination of model formulation, observations used to calibrate the semi-empirical models (for further discussion see, e.g., Rahmstorf et al., 2012; Moore et al., 2013; Church et al., 2013) and temperature pathways applied (Bittermann et al., 2017). While it is straightforward to compare published sea-level projections from the same emissions scenario knowing that differences will primarily be due to the sea-level model employed (Table 3) it is less straightforward for temperature because in addition to a range of sea-level models, different definitions and methods are used to obtain temperature pathways.

Schleussner et al. (2016) used a reduced complexity carbon-cycle/climate model to derive temperature ensembles keeping global mean temperature to below 1.5°C and below 2°C during the 21st century, each with 50% probability, and then projected GSL change using a temperature scaled sea-level model (Perrette

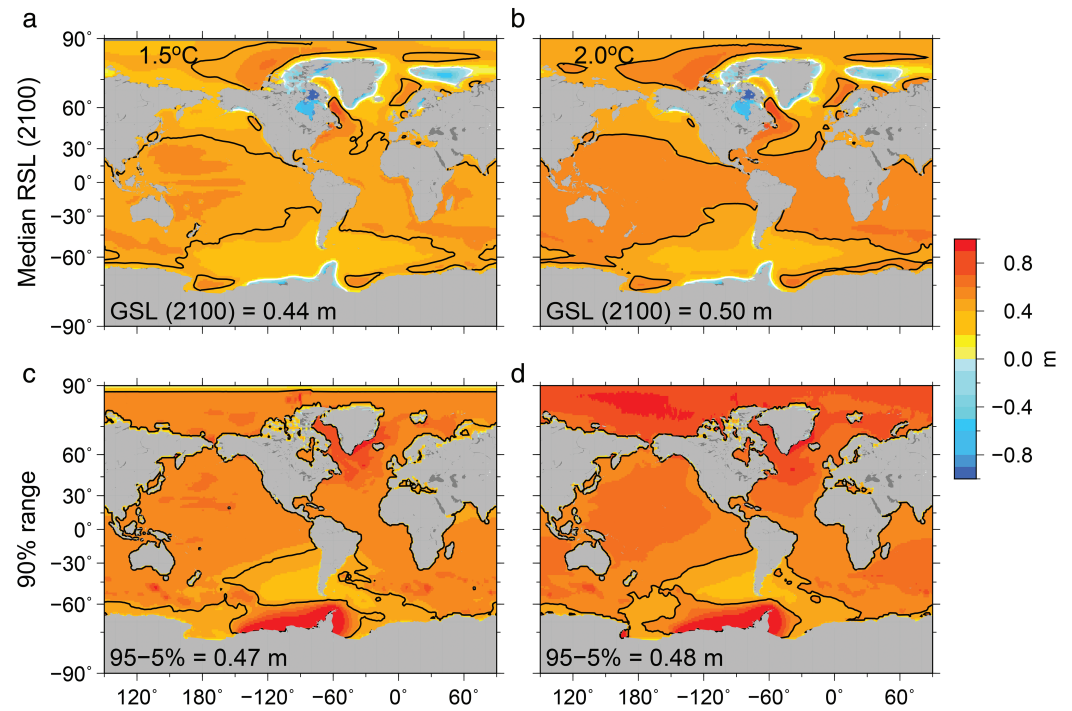


Figure 7. Median sea-level projections (a) and (b) and 90% range of uncertainty (c) and (d) for 1.5°C and 2°C temperature pathways in 2100 using process-based approach to calculate ice-sheet contributions. Black contour represents global average (labeled in each plot).

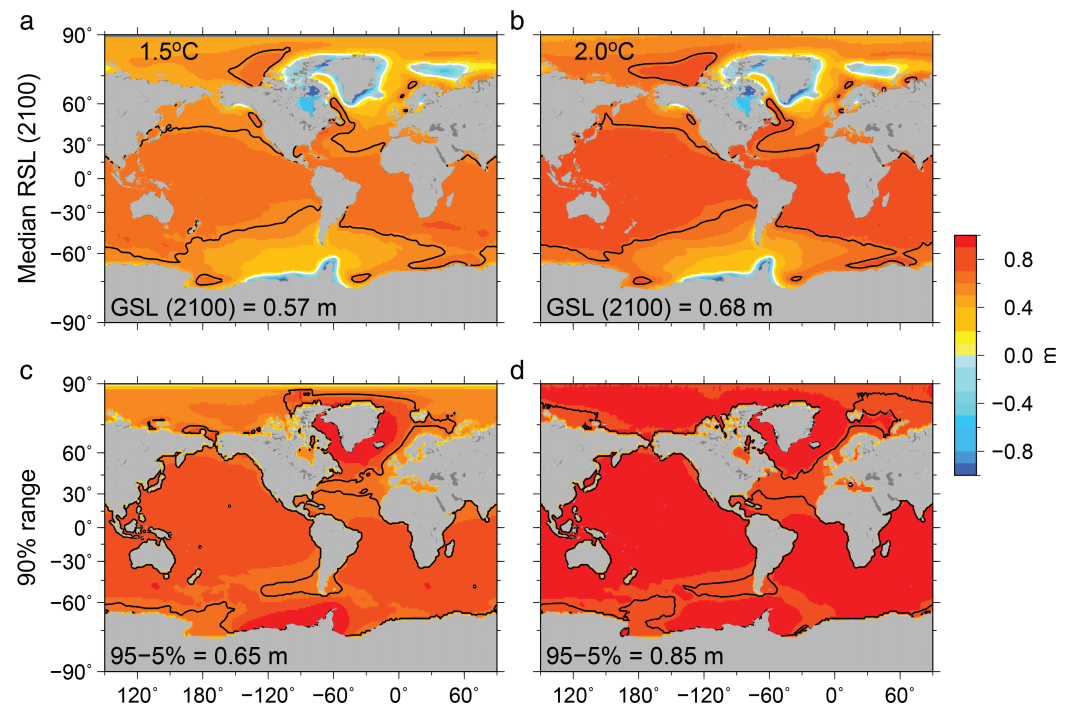


Figure 8. As in Figure 7 using semi-empirical approach to calculate ice-sheet contributions.

et al., 2013) with additional modifications to ice-sheet contributions. For the 1.5°C scenario, Bittermann et al. (2017) used a subsampled version of RCP 2.6 temperature outputs for a range of likelihoods of not exceeding 1.5°C with/without overshoot (in Table 2 we show 66% likelihood without overshoot) and for the 2°C scenario used idealized temperature pathways designed to stabilize at 2°C for a range of times (in Table 2 we show GSL for stabilization in 2080). Bittermann et al. (2017) then used the semi-empirical model by Kopp et al. (2016) to project GSL. Schaeffer et al. (2012) used temperature stabilization pathways with 40% and 50% chance of remaining below 1.5°C and 2°C in 2100 respectively, and then projected GSL using the semi-empirical model by Rahmstorf et al. (2012).

One of our key aims in using the semi-empirical approach is to explore uncertainty in future GSL projections and our results show a considerable overlap with the other published projections (Table 2). Our semi-empirical sea-level model (Grinsted et al., 2010), like others, is constrained by the sea-level/temperature behavior during the calibration period. We recognize that critical thresholds that have not been reached in the observational record will be unaccounted for in model projections, however these are more likely to be reached in far-future projections or high-end temperature scenarios (Bittermann et al., 2017) neither of which are relevant to our projections. Furthermore, many process-based models do not currently show large contributions from passing critical thresholds (e.g., Ritz et al. 2015), nor do advanced simulations indicate this in low-end scenarios (e.g., DeConto & Pollard, 2016).

In contrast to the research presented in Table 2, we also regionalize both process-based and semi-empirical projections by assuming the process-based global steric, glacier and land-water components are valid and that the residual GSL contribution represents the component from the ice sheets. This allows us to explore uncertainty in regional projections, which we expand upon in the following sections.

4.2. Sources of Uncertainty

The key unknown uncertainty in this analysis is a lack of process-based model simulations specifically targeted at 1.5°C and 2°C scenarios. In choosing to rely (though not exclusively) upon RCP 2.6, which implies

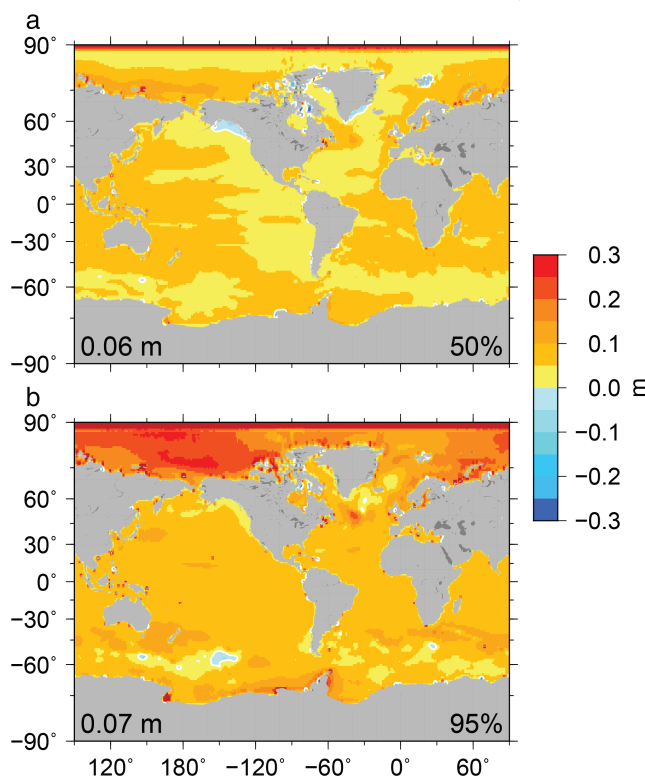


Figure 9. Difference between (a) median and (b) 95th percentile, projected regional sea-level in 2100 for 1.5°C and 2°C pathways using process-based approach to calculate ice-sheet contributions.

very strong mitigation, we assume ocean-mass redistribution and ice-sheet dynamics remain well behaved, in line with current estimates (Church et al., 2013) to inform us about the future state of sea level for these temperature thresholds.

The methodology we have taken is limited by the selection of models conforming to a temperature pathway within set limits. However, we have scaled the limits of each temperature pathway to be consistent with the uncertainty bounds for RCPs (Hartmann et al., 2013; Knutti et al., 2008; Stott & Kettleborough, 2002) and used a bootstrap technique to estimate the 95% level of 1 sigma uncertainty across models for each sea-level component (Figure S1 and description).

The information related to pathways is limited by the fact that our subsets of models are specific to two emission scenarios (RCP 2.6 and 4.5) with specified emissions pathways through the century (Moss et al., 2010) thus it is informative to compare our results

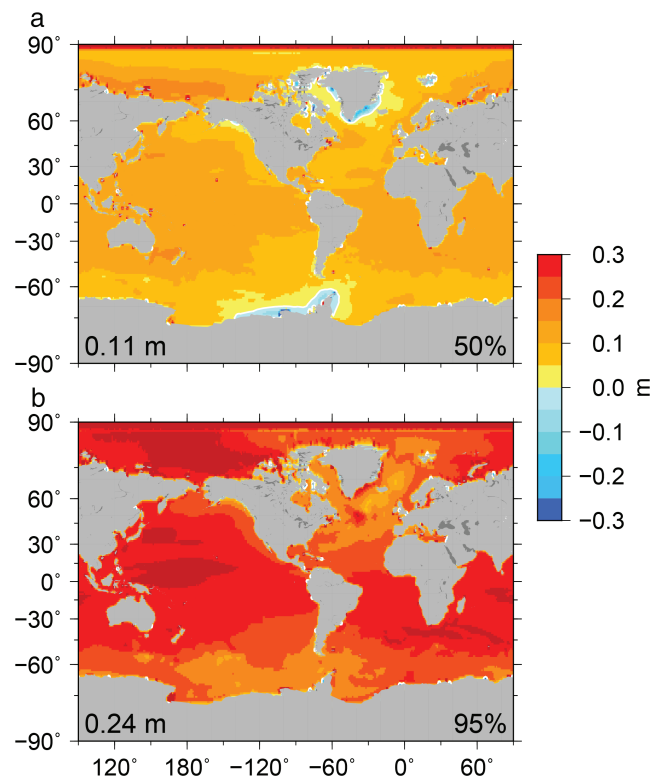


Figure 10. As in Figure 9 using semi-empirical approach to calculate ice-sheet contributions.

with projections for these scenarios (Tables 2 and 3, for completeness we recalculated GSL using Grinsted et al., 2010 with all available models for each RCP).

While the uncertainties estimated for our temperature scenarios are narrow (due to the specified temperature ranges) compared to RCPs (Tables 2 and 3: 67% range for 1.5/2.0°C: 0.24/0.4°C, for RCP 2.6/4.5: 1.4/1.5°C), the uncertainties of the process-based GSL for our temperature scenarios are close to those of the RCPs (Tables 2 and 3: 67% range for 1.5/2.0°C: 28/29 cm, for RCP 2.6/4.5: 33/35 cm). The similarity of GSL uncertainty ranges between our temperature scenarios and the RCPs shows that even a reduced subset of climate models, which are selected for their temperature pathways, display wide ranging behavior for other climate parameters.

A further source of uncertainty lays in the response time of individual components to the changes in temperature (or forcing). Mengel et al. (2016) modeled each component in a global semi-empirical model but underest-

imated 20th century GSL while 21st century projections under RCP 2.6 showed an underestimation of steric and glacier contributions and an overestimation of ice-sheet SMB and dynamics (particularly Greenland SMB) drawing total GSL closer to the process-based result (Table 3). Clearly more research is needed in this area and many of these component-based responses are likely to be distinct after 2100 (Church et al., 2013; Jevrejeva et al., 2012). For sea level, the key component illustrating this problem is the dynamical response of the ice sheets, which we discuss further in Section 4.3.

4.3. Dynamical Sea Level

While the two patterns of regional sea level are very similar, the bulk of these changes are driven by the range of dynamic sea-level (DSL) patterns from individual models driven by the two scenarios (Figures S2 and S3). It is clear that for the 1.5°C temperature pathway, MIROC5 (Watanabe et al., 2010) has enhanced DSL in most ocean basins (with the exception of the Southern Ocean) while CCSM4 (Gent et al., 2011) and BCC models (Wu et al., 2014) show little DSL response to temperature/scenario compared to other models. We also find this is the case for the 2°C temperature pathway where BCC models (Wu et al., 2014) show little DSL response but GISS-E2-R (Miller et al., 2014) shows strong DSL in the Arctic. Interestingly, MIROC5 and GISS-E2-R models require a sea-ice correction in the DSL component which we have performed and has been noted elsewhere (Landerer et al., 2013; Yin, 2012). MIROC5 gives unphysically low values of DSL in the Mediterranean, which we treat as an outlier in the solution of a multimodel ensemble mean. The Arctic enhancement of DSL is common for 2°C pathway models (14 out of 20 models) and to a lesser degree 1.5°C pathway models (6 out of 14 models).

4.4. Ice-Sheet Contributions

There remains a great deal of uncertainty surrounding the current state of the major ice sheets. While observational and model-based estimates of SMB have been reconciled, estimates of historical and present-day

Table 2.
Summary of Global Temperature and Sea-Level Projections to 2100 (Relative to 1986–2005) for 1.5°C and 2.0°C Scenarios

Reference	Scenario					
	1.5°C			2.0°C		
	Median	17–84	5–95	Median	17–84	5–95
Global surface temperature (°C) ^a						
This study	0.91	0.79–1.03		1.47	1.27–1.67	
Global sea-level (cm)						
Process-based						
This study	44	30–58	20–67	50	35–64	24–74
Schleussner et al. (2016) ^b	41	29–53		50	36–65	
Semi-empirical						
This study	57	40–77	28–93	68	47–93	32–117
Schaeffer et al. (2012) ^c	77		54–99	80		56–105
Bittermann et al. (2017) ^d	34		23–58	46		36–57

^aTemperature values averaged over 2081–2100.

^bSchleussner et al. (2016): idealized scenarios stabilizing below temperature thresholds during 21st century with 50% probability.

^cSchaeffer et al. (2012) use “MERGE400” and “Stab 2°C” scenarios with 40% and 50% chance of global mean temperature staying below 1.5°C and 2.0°C by 2100 respectively.

^dBittermann et al. (2017): 1.5°C scenario is subsampled RCP 2.6 with 66% likelihood of not exceeding 1.5°C without overshoot. 2.0°C scenario is idealized to stabilize in 2080.

dynamical ice sheet changes are limited, while projections are rare, primarily due to the complexity of the modeling problem. The physical mechanisms of dynamic ice sheet change include melt-water lubrication of the ice-sheet bed, increased ice stream flow after removal of buttressing ice shelves, ice cliff instability, bathymetry effects upon grounding line location, ocean ice-sheet interaction. Recent work by DeConto and Pollard (2016) introduced an ice-cliff failure mechanism and demonstrated in a calibrated ice-sheet model that projections of future Antarctic contributions varied widely between scenarios. Interestingly, under RCP 2.6, DeConto and Pollard (2016) find that contributions to sea level are small for two Pliocene calibration levels (11 ± 11 cm and 2 ± 13 cm by 2100). These are on the same order as the dynamic contribution to Antarctica estimated in IPCC AR5 (7 ± 9 cm, Church et al., 2013). Under RCP 4.5, DeConto and Pollard (2016) find contributions to sea level that are statistically significant from zero (49 ± 20 and 26 ± 28 cm by 2100). Since the lower third of RCP 4.5's temperature uncertainty range conforms to the 2°C threshold, this higher range of Antarctic contributions should not be neglected as in-compatible with either temperature pathway we use here, particularly 2°C. In fact, DeConto and Pollard (2016) state that an alteration to their model to allow higher Pliocene sea levels results in an RCP 2.6 projection of 16 ± 16 cm by 2100.

To place these model-based contributions into context, we identify where they lie within the PDF of Antarctic sea-level contribution of the expert elicitation by Bamber and Aspinall (2013). The RCP 2.6 projections lie between the 0th and 79th percentiles while RCP 4.5 projections lie between the 11th and 91st percentiles. Of course, the expert elicitation (Bamber & Aspinall, 2013) merged end-of-century rates based upon an end-of-century temperature range that was itself elicited. This means that the expert elicited rates were made according to the same experts end-of-century temperature estimate, whose perfect weights mean was 3.51°C (0.62–5.81°C) by 2100 relative to preindustrial from 2012 survey.

4.5. Vertical Land Motion

GIA, local tectonics, groundwater extraction and sediment compaction all impact vertical land motion at a range of spatial and temporal scales.

GIA is a global effect and is scenario independent. In this research we do not consider uncertainties associated with it because a limited number of models are available which we consider updates rather than parallel experiments. Each GIA field is the result of an inversion for both glacial ice sheet evolution and

Table 3.
Summary of Published Global Temperature and Sea-Level Projections in 2100 (Relative to 1986–2005) for RCP 2.6 and RCP 4.5 Scenarios

Reference	Scenario					
	RCP 2.6			RCP 4.5		
	Median	17–84	5–95	Median	17–84	5–95
Global surface temperature (°C) ^a						
IPCC (2013)	1.0	0.3–1.7		1.8	1.1–2.6	
Global sea-level (cm)						
Process-based						
IPCC (2013)	44	28–61		53	36–71	
Kopp et al. (2014)	50	37–65	29–82	59	45–77	36–93
Jackson and Jevrejeva (2016) ^b	44	29–58	16–68	54	36–72	22–85
Semi-empirical						
This study	59		28–101	69		30–122
Schaeffer et al. (2012)	75		52–96	90		64–121
Kopp et al. (2016)	38	28–51	24–61	51	39–69	33–85
Mengel et al. (2016)	39		28–56	53		37–77

^aTemperature values averaged over 2081–2100.

^bJackson and Jevrejeva (2016) did not originally publish projections for RCP 2.6, but we have applied identical methodology to give values here.

one-dimensional (1D) Earth structure conditioned on a range of geodetic observations (Peltier et al., 2015). While Slangen et al. (2014) recognize the scenario independence of GIA, they estimate systematic uncertainties by calculating the absolute difference between ICE5G (Peltier, 2004) and ANU (Nakada & Lambeck, 1988). These are small for the bulk of the global ocean, but are potentially more important close to former centers of deglaciation (e.g., US East coast see Fig. 2 in Slangen et al., 2014). Recently, Love et al. (2016) developed an approach similar to the climate community by estimating GIA fields for multiple glacial histories coupled to multiple 1D Earth structures in order to more accurately estimate GIA uncertainty along the Atlantic and Gulf coasts of North America.

Local tectonics, groundwater extraction and sediment compaction have increasingly local effects, beyond the resolution of our RSL projections. In many cases, the rates of vertical land motion associated with these effects exceed the magnitude of modern and future projected rates of sea-level change. If these rates are negative (that is the land is subsiding), then local sea-level will be locally amplified as evidenced today in mega cities like Jakarta and Manila (Deltares, 2013). Cities like Tokyo illustrate how local land motion can be altered by halting groundwater extraction, thus making local sea-level projections challenging. Furthermore, studies using Interferometric Synthetic Aperture Radar have revealed fine scale patterns of deformation from whole river-deltas (e.g., Erban et al., 2014) to street-by-street level in a city (e.g., Dixon et al., 2006). Planners and policy makers must identify the resolution of projections that are desirable for their needs and recognize the limitations of sea-level projections when applied to a given location.

5. Conclusions

We have used a novel approach to make global and regional sea-level projections by selecting climate model output based upon each models end-of-century global temperature falling within $1.5 \pm 0.21^\circ\text{C}$ or $2 \pm 0.28^\circ\text{C}$. We find that combinations of models from RCP 2.6 and RCP 4.5 provide GSL estimates (median and 5%–95% range) of 44 cm [20–67 m] and 50 cm [26–74 cm] in 2100 for 1.5°C or 2°C pathways. While these estimates use a conventional process-based approach, we also use a semi-empirical model to project GSL for each model-based temperature pathway to give GSL estimates of 58 cm (28–95 cm) and 68 cm (33–115 cm) by 2100 for 1.5°C or 2°C pathways.

Both of these approaches may underestimate contributions from Greenland and Antarctica, though the present knowledge indicates that low emissions scenarios (e.g., RCP 2.6), in line with an end-of-century temperature rise of 1.9°C, will contribute ~10 cm to GSL. It is pertinent to recognize that while a successful implementation of the Paris accord would significantly reduce potential sea-level rise by 2100, there will remain a commitment to sea-level rise beyond 2100 because of the equilibrium state sea-level will constantly try to reach. Jevrejeva et al. (2012) used the Grinsted et al. (2010) semi-empirical model conditioned upon radiative forcing rather than temperature to project GSL for RCP 2.6 and RCP 4.5 by 2500 of 53 cm (13–174 cm) and 184 cm (72–430 cm) while DeConto and Pollard (2016) projected to 2500 giving Antarctic contribution to GSL of 25 ± 23 and 569 ± 100 cm for RCP 2.6 and RCP 4.5, respectively. Further work clearly needs to be done to investigate the dynamic effects of ice sheets to improve projections, and in these strong mitigation scenarios the interaction between sea-level components needs to be clearly established as small changes to the underlying correlation structure will significantly alter uncertainties.

The research community has made scientifically rigorous projections of future climate change conditional upon scenarios to which conclusions about whether or not to implement strong mitigation are obvious. The commitments made in Paris were ground-breaking and revealed a political will for mitigation. One key question is the feasibility of implementing strong mitigation scenarios (e.g., RCP 2.6) to achieve a 2°C target (Anderson, 2015), which indicates the need for transformative technological innovation and globally affordable distribution (by no means a rapid process). However it is not a geophysical impossibility to achieve the Paris accord by 2100 with strengthened national commitments in 2030 followed by deep and rapid mitigation (Millar et al., 2017), though many economic sectors will require fundamental change to facilitate success (e.g., Wollenberg et al., 2016).

While half-a-degree warming sounds small, it matters (Schleussner et al., 2016, 2017). For sea level, the differences between 1.5°C and 2°C scenarios by 2100 are on the multi-centimeter scale and up to 20 cm in the right-hand tails of the probability distribution. Beyond 2100, projections of the future sea-level state for these two temperature scenarios will continue to (Church et al., 2013; Jevrejeva et al., 2012), though this is beyond the scope of this study. Future divergence is primarily due to the centennial response times of individual sea-level components to the changes in temperature (Church et al., 2013; Levermann et al., 2013). Further divergence between sea-level states at 1.5°C or 2°C may occur if the temperature threshold for Greenland ice sheet instability lies within these bounds, though the ice sheet tipping phase could last many hundreds of years (Lontzek et al., 2015; Robinson et al., 2012).

It is clear that achieving the Paris accord this century will reduce our long-term commitment to future sea-level rise over the next few centuries (DeConto & Pollard, 2016), tens of centuries (Levermann et al., 2013), and millennia (Clark et al., 2016). Naturally, decision makers have the infinitely more challenging job of identifying how best to achieve strong mitigation in the context of the UN's Sustainable Development Goals (UN, 2015b).

Acknowledgments

L.P.J. and S.J. were funded by the Natural Environmental Research Council under Grant Agreement No. NE/P01517/1 for the project called "Sea level rise trajectories by 2200 with warmings of 1.5 to 2°C". L.P.J. was concurrently funded by the Robertson Foundation (Grant No. 9907422). We acknowledge the World Climate Research Programme's Working Group on Coupled modeling for providing the CMIP5 archive and the climate modeling groups for providing their outputs. Furthermore, we acknowledge KNMI Climate Explorer (climexp.knmi.nl) for global average temperature projections processed from CMIP5 and Ben Marzeion for glacier mass-balance projections. We particularly thank Felix Pretis and Andrew Martinez useful discussions on the treatment of temperature uncertainties. We also thank two anonymous reviewers whose recommendations greatly improved the article. The global and regional sea-level projections presented here are available at climateeconometrics.org/sealevel.

References

- Anderson, K. (2015). Duality in climate science. *Nature Geoscience*, 8, 898–900. <https://doi.org/10.1038/ngeo2559>
- Bamber, J. L., & Aspinall, W. P. (2013). An expert judgement assessment of future sea level rise from the ice sheets. *Nature Climate Change*, 3, 424–427. <https://doi.org/10.1038/nclimate2998>.
- Bamber, J. L., & Riva, R. (2010). The sea level fingerprint of recent ice mass fluxes. *The Cryosphere*, 4, 621–627. <https://doi.org/10.5194/tc-4-621-2010>
- Bittermann, K., Rahmstorf, S., Kopp, R. E., & Kemp, A. C. (2017). Global mean sea-level rise in a world agreed upon in Paris. *Environmental Research Letters*, 12, 124010. <https://doi.org/10.1088/1748-9326/aa9def>
- Church, J. A., Clark, P. U., Cazenave, A., Gregory, J. M., Jevrejeva, S., Levermann, A., ... Unnikrishnan, A. S. (2013). Sea level change. In T. F. Stocker, D. Qin, G.-K. Plattner, M. Tignor, S. K. Allen, J. Boschung, et al. (Eds.), *Climate Change 2013: The Physical Science Basis. Contribution of Working Group I to the Fifth Assessment Report of the Intergovernmental Panel on Climate Change* (pp. 1137–1216). Cambridge, England and New York, NY: Cambridge University Press. <https://doi.org/10.1017/cb09781107415324.026>
- Clark, P. U., Shakun, J. D., Marcott, S. A., Mix, A. C., Eby, M., Kulp, S., ... Plattner, G.-K. (2016). Consequences of twenty-first-century policy for multi-millennial climate and sea-level change. *Nature Climate Change*, 6, 360–369. <https://doi.org/10.1038/nclimate2923>
- Climate Analytics (2017). *Ratification tracker*. Retrieved from <http://climateanalytics.org/hot-topics/ratificationtracker.html>
- Dalin, C., Wada, Y., Kastner, T., & Puma, M. J. (2017). Groundwater depletion embedded in international food trade. *Nature*, 543, 700–704. <https://doi.org/10.1038/nature21403>
- de Vries, H., Katsman, C., & Drijfhout, S. (2014). Constructing scenarios of regional sea level change using global temperature pathways. *Environmental Research Letters*, 9, 115007. <https://doi.org/10.1088/1748-9326/9/11/115007>
- DeConto, R. M., & Pollard, D. (2016). Contribution of Antarctica to past and future sea-level rise. *Nature*, 531, 591–597. <https://doi.org/10.1038/nature17145>

- Deltares (2013). *Sinking cities: An integrated approach towards solutions* (Tech. Rep.). Retrieved from <https://www.deltares.nl/app/uploads/2015/09/Sinking-cities.pdf>
- Dixon, T. H., Amelung, F., Ferretti, A., Novali, F., Rocca, F., Dokka, R., ... Whitman, D. (2006). Subsidence and flooding in New Orleans. *Nature*, 441, 587–588. <https://doi.org/10.1038/441587a>
- Erban, L. E., Gorelick, S. M., & Zebker, H. A. (2014). Groundwater extraction, land subsidence, and sea-level rise in the Mekong delta, Vietnam. *Environmental Research Letters*, 9, 084010. <https://doi.org/10.1088/1748-9326/9/8/084010>
- Farrell, W. E., & Clark, J. A. (1976). On postglacial sea level. *Geophysical Journal of the Royal Astronomical Society*, 46(3), 647–667.
- Fettweis, X., Franco, B., Tedesco, M., van Angelen, J. H., Lenaerts, J. T. M., van den Broeke, M. R., & Gallée, H. (2013). Estimating the Greenland ice sheet surface mass balance contribution to future sea level rise using the regional atmospheric climate model MAR. *The Cryosphere*, 7, 469–489. <https://doi.org/10.5194/tc-7-469-2013>
- Gent, P. R., Danabasoglu, G., Donner, L. J., Holland, M. M., Hunke, E. C., Jayne, S. R., ... Zhang, M. (2011). The community climate system model version 4. *Journal of Climate*, 24(19), 4973–4991. <https://doi.org/10.1175/2011JCLI4083.1>
- Grinsted, A., Jevrejeva, S., Riva, R. E. M., & Dahl-Jensen, D. (2015). Sea level rise projections for northern Europe under RCP8.5. *Climate Research*, 64, 15–23. <https://doi.org/10.3354/cr01309>
- Grinsted, A., Moore, J. C., & Jevrejeva, S. (2010). Reconstructing sea level from paleo and projected temperatures 200 to 2100 AD. *Climate Dynamics*, 34, 461–472. <https://doi.org/10.1007/s00382-008-0507-2>
- Hartmann, D. L., Tank, A. M. G. K., Rusticucci, M., Alexander, L. V., Brönnimann, S., Charabi, Y., ... Zhai, P. M. (2013). Observations: Atmosphere and surface. In T. F. Stocker, D. Qin, G.-K. Plattner, M. Tignor, S. K. Allen, J. Boschung, et al. (Eds.), *Climate Change 2013: The Physical Science Basis. Contribution of Working Group 1 to the Fifth Assessment Report of the Intergovernmental Panel on Climate Change* (pp. 159–254). Cambridge, England and New York, NY: Cambridge University Press. <https://doi.org/10.1017/cb09781107415324.007>
- Intergovernmental Panel on Climate Change (2013). Summary for policymakers, in *Climate Change 2013: The Physical Science Basis. Contribution of Working Group 1 to the Fifth Assessment Report of the Intergovernmental Panel on Climate Change*, edited by T. F. Stocker, D. Qin, G.-K. Plattner, M. Tignor, S. K. Allen, J. Boschung, A. Nauels, Y. Xia, V. Bex, and P. M. Midgley, pp. 1–30, Cambridge University Press, Cambridge, England and New York, NY. <https://doi.org/10.1017/cb09781107415324.004>
- Iversen, T., Bentsen, M., Bethke, I., Debernard, J. B., Kirkevåg, A., Selund, Ø., ... Seierstad, I. A. (2013). The Norwegian Earth system model, NorESM1-m—Part 2. Climate response and scenario projections. *Geoscientific Model Development*, 6(2), 389–415. <https://doi.org/10.5194/gmd-6-389-2013>
- Jackson, L. P., & Jevrejeva, S. (2016). A probabilistic approach to 21st century regional sea-level projections using RCP and high-end scenarios. *Global and Planetary Change*, 146, 179–189. <https://doi.org/10.1016/j.gloplacha.2016.10.006>
- Jevrejeva, S., Moore, J. C., & Grinsted, A. (2010). How will sea level respond to changes in natural and anthropogenic forcings by 2100? *Geophysical Research Letters*, 37, L07703. <https://doi.org/10.1029/2010GL042947>
- Jevrejeva, S., Moore, J. C., & Grinsted, A. (2012). Sea level projections to AD2500 with a new generation of climate change scenarios. *Global and Planetary Change*, 80–81, 14–20. <https://doi.org/10.1016/j.gloplacha.2011.09.006>
- Knutti, R. (2010). The end of model democracy? *Climatic Change*, 102(3–4), 395–404. <https://doi.org/10.1007/s10584-010-9800-2>
- Knutti, R., Allen, M. R., Friedlingstein, P., Gregory, J. M., Hegerl, G. C., Meehl, G. A., ... Wigley, T. M. L. (2008). A review of uncertainties in global temperature projections over the twenty-first century. *Journal of Climate*, 21, 2651–2663. <https://doi.org/10.1175/2007JCLI2119.1>
- Kopp, R. E., Horton, R. M., Little, C. M., Mitrovica, J. X., Oppenheimer, M., Rasmussen, D. J., ... Tebaldi, C. (2014). Probabilistic 21st and 22nd century sea-level projections at a global network of tide-gauge sites. *Earth's Future*, 2, 383–406. <https://doi.org/10.1002/2014ef000239>
- Kopp, R. E., Kemp, A. C., Bittermann, K., Horton, B. P., Donnelly, J. P., Gehrels, W. R., ... Rahmstorf, S. (2016). Temperature-driven global sea-level variability in the common era. *Proceedings of the National Academy of Sciences of the United States of America*, 113, 1413–1441. <https://doi.org/10.1073/pnas.1517056113>
- Landerer, F. W., Gleckler, P. J., & Lee, T. (2013). Evaluation of CMIP5 dynamic sea surface height multi-model simulations against satellite observations. *Climate Dynamics*, 43, 1271–1283. <https://doi.org/10.1007/s00382-013-1939-x>
- Landerer, F. W., Jungclaus, J. H., & Marotzke, J. (2007). Regional dynamic and steric sea level change in response to the IPCC-A1b scenario. *Journal of Physical Oceanography*, 37(2), 296–312. <https://doi.org/10.1175/JPO3013.1>
- Le Bars, D., Drijfhout, S., & de Vries, H. (2017). A high-end sea level rise probabilistic projection including rapid Antarctic ice sheet mass loss. *Environmental Research Letters*, 12, 044013. <https://doi.org/10.1088/17489326/aa6512>
- Le Cozannet, G., Manceau, J.-C., & Rohmer, J. (2017). Bounding probabilistic sea-level projections within the framework of the possibility theory. *Environmental Research Letters*, 12, 014012. <https://doi.org/10.1088/1748-9326/aa5528>
- Lenaerts, J. T. M., van den Broeke, M. R., van de Berg, W. J., van Meijgaard, E., & Kuipers Munneke, P. (2012). A new, high-resolution surface mass balance map of Antarctica (1979–2010) based on regional atmospheric climate modeling. *Geophysical Research Letters*, 39(4), L04501. <https://doi.org/10.1029/2011GL050713>
- Levermann, A., Clark, P. U., Marzeion, B., Milne, G. A., Pollard, D., Radic, V., & Robinson, A. (2013). The multimillennial sea-level commitment of global warming. *Proceedings of the National Academy of Sciences of the United States of America*, 110, 13745–13750. <https://doi.org/10.1073/pnas.1219414110>
- Lontzek, T. S., Cai, Y., Judd, K. L., & Lenton, T. M. (2015). Stochastic integrated assessment of climate tipping points indicates the needs for strict climate policy. *Nature Climate Change*, 5, 441–444. <https://doi.org/10.1038/nclimate2570>
- Love, R., Milne, G. A., Tarasov, L., Engelhart, S. E., Hijma, M. P., Latychev, K., ... Törnqvist, T. E. (2016). The contribution of glacial isostatic adjustment to projections of sea-level change along the Atlantic and Gulf coasts of North America. *Earth's Future*, 4, 440–464. <https://doi.org/10.1002/2016EF000363>
- Marzeion, B., Jarosch, A. H., & Hofer, M. (2012). Past and future sea-level change from the surface mass balance of glaciers. *The Cryosphere*, 6, 1295–1322. <https://doi.org/10.5194/tc-6-1295-2012>
- Massey, F. J. (1951). The Kolmogorov-Smirnov test for goodness of fit. *Journal of the American Statistical Association*, 46(253), 68–78. <https://doi.org/10.1080/01621459.1951.10500769>
- Mengel, M., Levermann, A., Frieler, K., Robinson, A., Marzeion, B., & Winkelmann, R. (2016). Future sea level rise constrained by observations and long-term commitment. *Proceedings of the National Academy of Sciences of the United States of America*, 113, 2597–2602. <https://doi.org/10.1073/pnas.1500515113>
- Millar, R. J., Fuglestad, J. S., Friedlingstein, P., Rogelj, J., Grubb, M. J., Matthews, H. D., ... Allen, M. R. (2017). Emission budgets and pathways consistent with limiting warming to 1.5°C. *Nature Geoscience*, 10, 741–747. <https://doi.org/10.1038/ngeo3031>
- Miller, R. L., Schmidt, G. A., Nazarenko, L. S., Tausnev, N., Bauer, S. E., DelGenio, A. D., ... Zhang, J. (2014). CMIP5 historical simulations (1850–2012) with GISS model 2. *Journal of Advances in Modeling Earth Systems*, 6(2), 441–478. <https://doi.org/10.1002/2013MS000266>

- Mitchell, D., AchutaRao, K., Allen, M., Bethke, I., Beyerle, U., Ciavarella, A., ... Zaaboul, R. (2017). Half a degree additional warming, prognosis and projected impacts (HAPPI): Background and experimental design. *Geoscientific Model Development*, 10(2), 571–583. <https://doi.org/10.5194/gmd-10-571-2017>
- Mitrovica, J. X., Gomez, N., Morrow, E., Hay, C., Latychev, K., & Tamisiea, M. E. (2011). On the robustness of predictions of sea level fingerprints. *Geophysical Journal International*, 187, 729–742. <https://doi.org/10.1111/j.1365-246X.2011.05090.x>
- Moore, J. C., Grinsted, A., Zwinger, T., & Jevrejeva, S. (2013). Semi-empirical and process-based global sea level projections. *Reviews of Geophysics*, 51(3), 484–522. <https://doi.org/10.1002/rog.20015>
- Moss, R. H., Edmonds, J. A., Hibbard, K. A., Manning, M. R., Rose, S. K., Vuuren, D. P. V., ... Wilbanks, T. J. (2010). The next generation of scenarios for climate change research and assessment. *Nature*, 463(7282), 747–756. <https://doi.org/10.1038/nature08823>
- Nakada, M., & Lambeck, K. (1988). The melting history of the late Pleistocene Antarctic ice sheet. *Nature*, 333(5), 36–40. <https://doi.org/10.1038/333036a0>
- Naueis, A., Meinshausen, M., Mengel, M., Lorbacher, K., & Wigley, T. M. L. (2017). Synthesizing long term sea level rise projections—The MAGICC sea level model v2.0. *Geoscientific Model Development*, 10, 2495–2524. <https://doi.org/10.5194/gmd-10-2495-2017>
- Peltier, W. R. (2004). Global glacial isostasy and the surface of the ICE-age Earth: The ICE-5G (VM2) model and GRACE. *Annual Review of Earth and Planetary Sciences*, 32, 111–149. <https://doi.org/10.1146/annurev.earth.32.082503.144359>
- Peltier, W. R., Argus, D. F., & Drummond, R. (2015). Space geodesy constrains ICE age terminal deglaciation: The global ICE-6G_C (VM5a) model. *Journal of Geophysical Research—Solid Earth*, 119, 450–487. <https://doi.org/10.1002/2014JB011176>
- Perretre, M., Landerer, F., Riva, R., Frieler, K., & Meinshausen, M. (2013). A scaling approach to project regional sea level rise and its uncertainties. *Earth System Dynamics*, 4, 11–29. <https://doi.org/10.5194/esd-4-11-2013>
- Rahmstorf, S., Perretre, M., & Vermeer, M. (2012). Testing the robustness of semi-empirical sea level projections. *Climate Dynamics*, 39, 861–875. <https://doi.org/10.1007/s00382-011-1226-7>
- Rasmussen, D. J., Bittermann, K., Buchanan, M., Kulp, S., Strauss, B., Kopp, R. E., & Oppenheimer, M. (2017). *Coastal flood implications of 1.5°C, 2.0°C, and 2.5°C temperature stabilization targets in the 21st and 22nd century*. Retrieved from <https://arxiv.org/abs/1710.08297v1>
- Richter, K., Riva, R. E. M., & Drange, H. (2013). Impact of self-attraction and loading effects induced by shelf mass loading on projected regional sea level rise. *Geophysical Research Letters*, 40, 1144–1148. <https://doi.org/10.1002/grl.50265>
- Ritz, C., Edwards, T. L., Durand, G., Payne, A. J., Peyaud, V., & Hindmarsh, R. C. A. (2015). Potential sea-level rise from Antarctic ice-sheet instability constrained by observations. *Nature*, 528, 115–118. <https://doi.org/10.1038/nature16147>
- Robinson, A., Calov, R., & Ganopolski, A. (2012). Multistability and critical thresholds of the Greenland ice sheet. *Nature Climate Change*, 2, 429–432. <https://doi.org/10.1038/nclimate1449>
- Rogelj, J., den Elzen, M., Höhne, N., Fransen, T., Fekete, H., Winkler, H., ... Meinshausen, M. (2016). Paris agreement climate proposals need a boost to keep warming well below 2°C. *Nature*, 534, 631–639. <https://doi.org/10.1038/nature18307>
- Schaeffer, M., Hare, W., Rahmstorf, S., & Vermeer, M. (2012). Long-term sea-level rise implied by 1.5°C and 2°C warming levels. *Nature Climate Change*, 2, 867–870. <https://doi.org/10.1038/nclimate1584>
- Schleussner, C.-F., Lissner, T. K., Fischer, E. M., Wohland, J., Perretre, M., Golly, A., ... Schaeffer, M. (2016). Differential climate impacts for policy-relevant limits to global warming: The case of 1.5°C and 2°C. *Earth System Dynamics*, 7, 327–351. <https://doi.org/10.5194/esd-7-327-2016>
- Schleussner, C.-F., Pfeleiderer, P., & Fischer, E. M. (2017). In the observational record half a degree matters. *Nature Climate Change*, 7, 460–462. <https://doi.org/10.1038/nclimate3320>
- Shepherd, A., Ivins, E. R., Geruo, A., Barletta, V. R., Bentley, M. J., Bettadpur, S., ... Zwally, H. J. (2012). A reconciled estimate of ice-sheet mass balance. *Science*, 338, 1183–1189. <https://doi.org/10.1126/science.1228102>
- Slangen, A. B. A., Carson, M., Katsman, C. A., van de Wal, R. S. W., Köhl, A., Vermeersen, L. L. A., & Stammer, D. (2014). Projecting twenty-first century regional sea-level changes. *Climatic Change*, 124, 317–332. <https://doi.org/10.1007/s10584-014-1080-9>
- Stott, P. A., & Kettleborough, J. A. (2002). Origins and estimates of uncertainty in predictions of twenty-first century temperature rise. *Nature*, 416, 723–726. <https://doi.org/10.1038/416723a>
- Taylor, K. E., Stouffer, R. J., & Meehl, G. E. (2012). An overview of CMIP5 and the experiment design. *Bulletin of the American Meteorological Society*, 93, 485–498. <https://doi.org/10.1175/bams-d-11-00094.1>
- United Nations (2015a). *Adoption of the Paris agreement* (Tech. Rep. FCCC/CP/2015/L.9/Rev.1). United Nations Framework Convention on Climate Change. Retrieved from <http://www.un.org/en/ga/search/viewdoc.asp?symbol=FCCC/CP/2015/L.9/Rev.1>
- United Nations (2015b). *Transforming our world: The 2030 agenda for sustainable development* (Tech. Rep. A/RES/70/1). United Nations General Assembly. Retrieved from <http://www.un.org/en/ga/search/viewdoc.asp?symbol=A/RES/70/1>
- Vermeer, M., & Rahmstorf, S. (2009). Global sea level linked to temperature. *Proceedings of the National Academy of Sciences of the United States of America*, 106(21), 527–21, 532. <https://doi.org/10.1073/pnas.0907765106>
- Wada, Y., Reager, J. T., Chao, B. J., Wang, J., Lo, M.-H., Song, C., ... Gardner, A. S. (2017). Recent changes in land water storage and its contribution to sea level variations. *Surveys in Geophysics*, 38, 131–152. <https://doi.org/10.1007/s10712-016-9399-6>
- Watanabe, M., Suzuki, T., Oishi, R., Komuro, Y., Watanabe, S., Emori, S., ... Kimoto, M. (2010). Improved climate simulation by MIROC5: Mean states, variability, and climate sensitivity. *Journal of Climate*, 23(23), 6312–6335. <https://doi.org/10.1175/2010JCLI3679.1>
- Wollenberg, E., Richards, M., Smith, P., Havlik, P., Obersteiner, M., Tubiello, F. N., ... Campbell, B. M. (2016). Reducing emissions from agriculture to meet the 2°C target. *Global Change Biology*, 22, 3859–3864. <https://doi.org/10.1111/gcb.13340>
- Wu, T., Song, L., Li, W., Wang, Z., Zhang, H., Xin, X., ... Zhou, M. (2014). An overview of BCC climate system model development and application for climate change studies. *Journal of Meteorological Research*, 28(1), 4–56. <https://doi.org/10.1007/s13351-014-3041-7>
- Yin, J. (2012). Century to multi-century sea level rise projections from CMIP5 models. *Geophysical Research Letters*, 39, L17709. <https://doi.org/10.1029/2012gl052947>
- Yin, J., Griffies, S. M., & Stouffer, R. J. (2010). Spatial variability of sea level rise in twenty-first century projections. *Journal of Climate*, 23, 4585–4607. <https://doi.org/10.1175/2010JCLI3533.1>